Journal of Biomechanics 48 (2015) 449–455

Contents lists available at ScienceDirect

Journal of Biomechanics

journal homepage: www.elsevier.com/locate/jbiomech
www.JBiomech.com

# Biomechanical risk factors and flexor tendon frictional work in the cadaveric carpal tunnel

Aaron M. Kociolek, Jimmy Tat, Peter J. Keir *

*Department of Kinesiology, McMaster University, Hamilton, Ontario, Canada*

ARTICLE INFO

*Article history:*
Accepted 8 December 2014

*Keywords:*
Carpal tunnel
Tendon
Subsynovial connective tissue
Gliding resistance
Viscoelastic

ABSTRACT

Pathological changes in carpal tunnel syndrome patients include fibrosis and thickening of the subsynovial connective tissue (SSCT) adjacent to the flexor tendons in the carpal tunnel. These clinical findings suggest an etiology of excessive shear-strain force between the tendon and SSCT, underscoring the need to assess tendon gliding characteristics representative of repetitive and forceful work. A mechanical actuator moved the middle finger flexor digitorum superficialis tendon proximally and distally in eight fresh frozen cadaver arms. Eighteen experimental conditions tested the effects of three well-established biomechanical predictors of injury, including a combination of two wrist postures (0° and 30° flexion), three tendon velocities (50, 100, 150 mm/sec), and three forces (10, 20, 40 N). Tendon gliding resistance was determined with two light-weight load cells, and integrated over tendon displacement to represent tendon frictional work. During proximal tendon displacement, frictional work increased with tendon velocity (58.0% from 50–150 mm/sec). There was a significant interaction between wrist posture and tendon force. In wrist flexion, frictional work increased 93.0% between tendon forces of 10 and 40 N. In the neutral wrist posture, frictional work only increased 33.5% (from 10–40 N). During distal tendon displacement, there was a similar multiplicative interaction on tendon frictional work. Concurrent exposure to multiple biomechanical work factors markedly increased tendon frictional work, thus providing a plausible link to the pathogenesis of work-related carpal tunnel syndrome. Additionally, our study provides the conceptual basis to evaluate injury risk, including the multiplicative repercussions of combined physical exposures.



## 1. Introduction

Carpal tunnel syndrome (CTS) is a peripheral entrapment neuropathy due to compression of the median nerve at the wrist. While the etiology of CTS is multi-factorial (Staal et al., 2007), common histopathologic changes include fibrosis and thickening of the subsynovial connective tissue (SSCT) surrounding the flexor tendons in the carpal tunnel (Barr et al., 2004; Ettema et al., 2006; Jinrok et al., 2004). The SSCT loosely attaches the flexor tendons to the visceral synovium, and is comprised of collagen bundles that form adjacent layers interconnected by small perpendicular fibrils. During flexor tendon displacement, the SSCT is strained, with deep layers close to tendon moving before superficial layers near the visceral synovium (Guimberteau et al., 2010). Repetitive tendon motion is thought to promote shear damage at the tendon-SSCT interface, which is supported by the finding that fibrosis is exacerbated in SSCT layers adjacent to flexor tendon (Ettema et al., 2006; Schuind et al., 1990).

Moore et al. (1991) used 12 biomechanical measures to model tissue loads in the wrist/hand and found that flexor tendon frictional work was the best predictor of injury. Tanaka and McGlothlin (1993) also developed a heuristic model of the wrist using frictional energy to predict work-related CTS. Both of these methods utilized the well-established belt-pulley model that likens a tendon gliding over a curved surface, such as the transverse carpal ligament in wrist flexion, to a belt around a pulley (Armstrong and Chaffin, 1979). Keir and Wells (1999) determined the radius of tendon curvature in the carpal tunnel decreased with both wrist flexion angle and tendon force magnitude thereby increasing normal stress on the median nerve in addition to the effect of tendon tension on contact stress.

More recently, flexor tendon gliding resistance was experimentally measured (in vitro) within the carpal tunnel (Filius et al., 2014; Zhao et al., 2007). Zhao et al. (2007) found that tendon gliding resistance increased exponentially with tendon displacement, primarily due to the viscoelastic SSCT. The researchers also quantified the effect of wrist flexion angle on tendon gliding resistance; however, the slow test velocity of 2 mm/sec likely diminished viscoelastic shear-strain. There

* Correspondence to: Department of Kinesiology, McMaster University, 1280 Main Street West, Hamilton, Ontario, Canada L8S 4K1. Tel.: +905 525 9140 x23543; fax: +905 523 6011.
*E-mail address:* pjkeir@mcmaster.ca (P.J. Keir).

http://dx.doi.org/10.1016/j.jbiomech.2014.12.029
0021-9290/

remains a need to quantify tendon gliding characteristics representative of repetitive and forceful work to better understand the interplay between contact shear with other anatomical structures and tenosynovial resistance on overall friction in the carpal tunnel.

The purpose of this study was to quantify flexor tendon gliding resistance and frictional work in two wrist postures (0° and 30° flexion), three tendon velocities (50 mm/sec, 100 mm/sec, 150 mm/sec), and three tendon forces (10 N, 20 N, 40 N). We hypothesized that greater physical exposure, including higher tendon velocity and force, would increase flexor tendon frictional work, especially with wrist flexion.

## 2. Methods

### 2.1. Cadaveric specimens

Eight unmatched fresh frozen human cadaver upper limbs were amputated at the mid-humerus (age 56.6 ± 15.5 yr, height 178.4 ± 8.8 cm, mass 99.7 ± 26.2 kg). Exclusion criteria included a known history of wrist tendinopathy, peripheral nerve disease, and CTS. This study was approved by the Hamilton Integrated Research Ethics Board.

Specimens were thawed at 5 °C for approximately 12 h prior to dissection. The flexor digitorum profundus (FDP) and flexor digitorum superficialis (FDS) tendons were exposed on both proximal and distal sides of the transverse carpal ligament. Passive finger flexion/extension movements were used to identify all four tendons of FDP and FDS. The flexor pollicis longus (FPL) tendon and median nerve were also identified. The finger and thumb flexor tendons and median nerve were excised from the proximal and distal attachments. The carpal tunnel was left undisturbed and the mid-humeral amputation ensured that the ulna and radius remained intact to preserve anatomic fidelity of the wrist complex.

### 2.2. Testing apparatus

Upper limb specimens were secured to the testing apparatus at the proximal forearm with an adjustable clamp as well as the distal forearm (proximal to the wrist crease), hand (3rd metacarpal), and middle finger (3rd distal phalanx) with plastic fasteners (Fig. 1). The testing apparatus was hinged at the wrist to change the joint angle in the experiment. The middle finger FDS tendon was attached proximally to a cable, connected to a linear actuator (ERC3, IAI America Inc., Torrance, CA) through a series of mechanical pulleys. Distally, the tendon was fixed to a cable that curved around a pulley and attached to a constant force spring (N-series, Vulcan Spring Co, Telford, PA). Both sides of the tendon were attached directly to cable ends with 6 mm aluminum crimping sleeves. Two light-weight load cells (LCM-200, Futek Inc., Irvine, CA) were connected in series with the tendon proximal and distal to the carpal tunnel. A pulley on the proximal side of the carpal tunnel was also instrumented with a rotary potentiometer (6370 Series, State Electronics Corp., East Hanover, NJ) to calculate displacement of the tendon via the motor.

The proximal ends of the remaining finger flexor tendons (3 FDS and 4 FDP) were connected to an adjustable plate on the testing apparatus. Distally, the tendons were fixed to extension springs to maintain a tension of 250 g. The extension springs connected to another adjustable plate to preserve the tendon lines of action through the carpal tunnel. Since the FPL was only exposed and excised from the origin site, the tendon was fixed to an extension spring on the proximal side of the carpal tunnel while the thumb was secured to the testing apparatus. The distal median nerve branches throughout the hand; thus, tension was provided with an extension spring on the proximal side of the testing apparatus.

### 2.3. Experimental protocol

FDS tendon displacements of the middle finger were produced with the linear actuator. The motor was programmed to move 30 mm proximally and distally to represent tendon displacements for full finger flexion and extension, respectively (Kociolek and Keir, 2013). Each specimen was preconditioned with twenty-four continuous tendon displacement cycles (velocity 50 mm/sec; force 10 N). Tendon displacements were tested in eighteen conditions using combinations of two wrist postures (0° and 30° flexion), three tendon velocities (50, 100, 150 mm/sec), and three tendon forces supplied by constant force springs (~ 10, 20, 40 N). While the springs produce constant force with greater deflections, we anticipated different magnitudes for proximal versus distal tendon displacements, due to friction of the mounting axle (Williams et al., 2013). Spring forces were 25.4% lower for distal deflections compared to proximal deflections (Table 1). *Note*: from herein we will refer to the tendon forces based on the spring specifications for ease of reading (10, 20, 40 N).

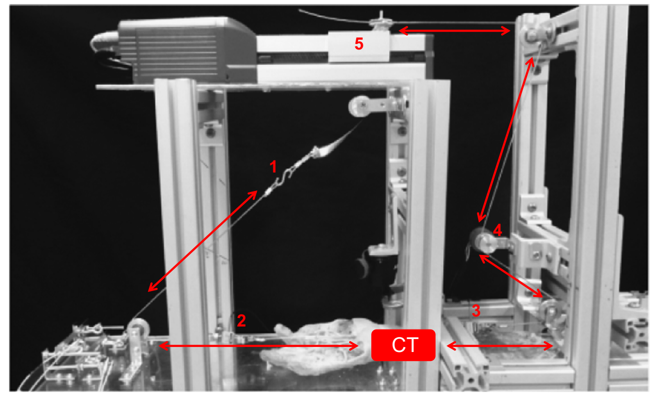


**Fig. 1.** A cadaver specimen in the testing apparatus. Gliding characteristics of the middle finger FDS tendon were evaluated as a motor moved the tendon proximally (finger flexion) and distally (finger extension). The apparatus includes the (1) constant force spring, (2) distal load cell, (3) proximal load cell, (4) rotary potentiometer, and (5) linear actuator. Note: the remaining flexor tendons and median nerve are not yet connected so that all the components of the apparatus are clearly visible.

**Table 1**
Mean ( ± standard error of mean) distal tendon force measurements from the constant force springs during proximal and distal tendon displacement.

| Manufactured rating (N) | Prox disp (N) | Dist disp (N) |
|---|---|---|
| 10 *N* | 9.52 ± 0.12 | 6.39 ± 0.11 |
| 20 *N* | 21.93 ± 0.28 | 16.00 ± 0.20 |
| 40 *N* | 39.12 ± 0.62 | 30.24 ± 0.37 |

*10 N, 20 N, and 40 N – Expected force magnitude of the constant force springs from manufacturer specifications.

Four proximal-distal tendon displacement cycles were tested in each experimental condition, for a total of 72 cycles (18 conditions × 4 cycles/condition). A balanced design mitigated order effects for wrist posture (i.e. four cadavers started in the neutral posture, four cadavers started in the flexed posture). Tendon force was randomized for each wrist posture, and tendon velocity was block randomized within each force level. The specimens were lightly sprayed with saline solution before starting each wrist posture block. While this represents minimal spraying, the potential for confounded results due to changes in lubrication were minimized (Uchiyama et al., 1997).

Tendon velocities and forces in this study were similar to previous in vivo studies. Tendons have been shown to reach velocities up to 150 mm/sec during full finger flexion (Tat et al., 2013). Unrestricted dynamic finger tapping produces tendon force between 8–17 N, with higher magnitudes during forceful exertions (Dennerlein, 2005). The impact of wrist posture on tendon friction is well established (Armstrong and Chaffin, 1979; Tanaka and McGlothlin, 1993; Zhao et al., 2007). Representing wrist flexion in vitro required meticulous care since the tendons were detached on both sides of the carpal tunnel. During wrist flexion trials, the flexor tendons were displaced 10 mm in the proximal direction to represent the position of the tendon for an intact musculotendon unit (Armstrong and Chaffin, 1978).

### 2.4. Data collection and analysis

Middle finger FDS tendon forces and displacements were collected at 120 Hz (LabView 8.5, National Instruments Corp., Austin, TX). Load cell and potentiometer data were smoothed with a dual second-order low pass Butterworth filter ($f_c$=6 Hz). Tendon gliding resistance was defined as the difference between proximal and distal tendon forces ($F_p$ – $F_d$). Positive gliding resistance represented resistance to proximal tendon displacement while negative gliding resistance represented resistance to distal tendon displacement. Tendon frictional work was calculated by integrating tendon gliding resistance over tendon displacement in both the proximal and distal displacement phase of each cycle.

### 2.5. Statistical analysis

Due to acceleration and deceleration of the motor, the first 5 mm and last 5 mm of proximal tendon displacement were removed to ensure constant velocity. Thus, we determined tendon gliding resistance for 20 mm of displacement (5–25 mm). A smaller displacement interval was used for return distal tendon displacement,